Applied Surface Science 540 (2021) 148264

Contents lists available at ScienceDirect

Applied Surface Science

journal homepage: www.elsevier.com/locate/apsusc

The structures and thermoelectric properties of Zn-Sb alloy films fabricated by electron beam evaporation through an ion beam assisted deposition

Shih-Chieh Hsu [a,1], Jhen-Yong Hong [b,1], Cheng-Lung Chen [c,1], Sheng-Chi Chen [d,e,*], Jia-Han Zhen [d], Wen-Pin Hsieh [f], Yang-Yuan Chen [c], Tung-Han Chuang [g,*]

[a] Department of Chemical and Materials Engineering, Tamkang University, New Taipei City 251, Taiwan
[b] Department of Physics, Tamkang University, New Taipei City 251, Taiwan
[c] Institute of Physics, Academia Sinica, Taipei 11529, Taiwan
[d] Department of Materials Engineering and Center for Plasma and Thin Film Technologies, Ming Chi University of Technology, New Taipei City 243, Taiwan
[e] College of Engineering and Center for Green Technology, Chang Gung University, Taoyuan 333, Taiwan
[f] Institute of Earth Sciences, Academia Sinica, Taipei 11529, Taiwan
[g] Institute of Materials Science and Engineering, National Taiwan University, Taipei 106, Taiwan

ARTICLE INFO

Keywords:
Zn-Sb film
Ion beam assisted deposition
Seebeck coefficient
Thermoelectric properties

ABSTRACT

Zn-Sb alloys are potential low-cost and non-toxic p-type thermoelectric materials for applications in the temperature range between 300 and 700 K. In this experiment, Zn-Sb alloy films were prepared by electron beam evaporation through an ion beam assisted deposition (IBAD). Our studies have confirmed that the structural phase, chemical composition, chemical binding, carrier concentration and microstructures of the film can indeed be effectively controlled by the voltage and current of the ion beam. Particularly, the carrier concentration of the film will rise along with the increase of the argon ion beam current. When the ion beam currents are set at 0.2–0.6 A, the carrier concentrations of the films can be controlled at around 10^{19}–10^{20} cm^{-3}, which fall within the optimal carrier concentration range for Zn-Sb based thermoelectric materials. The temperature dependence of Seebeck coefficient and the electrical conductivity of the films were measured to evaluate their thermoelectric performance. The results indicate that the film with Zn_4Sb_3 + ZnSb mixed phase will have better thermoelectric properties. A high power factor value of ~1280 μW/m-K^2 is obtained in the films assisted by the ion beam current of 0.6 A. Our results demonstrate that the IBAD technique is extraordinary promising to fabricate Zn-Sb films with excellent thermoelectric performance and can be used to produce other potential thermoelectric materials.

1. Introduction

Recently, the rising demand for thermoelectric (TE) materials with high conversion efficiency have attracted much attention in the fields of device applications and materials science [1–3]. While previous researchers focused on bulk materials for high-power applications [4,5], researchers in recent years put an emphasis on low-power applications of sensors and devices based on the thin film and micro devices techniques [6–8]. However, the main challenge that prevents TE materials from being widely used is its relatively low thermoelectric conversion efficiency, which is usually evaluated by the figure of merit, $ZT = \sigma S^2 T/\kappa$, where σ is the electrical conductivity, *S* is the Seebeck coefficient, T is the absolute temperature, κ is the thermal conductivity consisting of a contribution from the charge carrier κ_e and the lattice κ_L. σS^2 is known as the power factor (*PF*). Obviously, potential TE materials should have both a high Seebeck coefficient and a high σ/κ ratio. Over the past decades, several promising strategies such as thin film engineering [1,9], hierarchical structuring [10] and band structure engineering [11] have been developed to overcome this challenge by reducing thermal conductivity and/ or enhancing the power factor to increase ZT.

Owing to the growing interest in self-powered microelectronic systems, TE films have recently played an important role in the development of various miniaturized thermoelectric systems [12,13]. Many techniques, including electrochemical deposition, co-evaporation

* Corresponding authors at: Department of Materials Engineering and Center for Plasma and Thin Film Technologies, Ming Chi University of Technology, New Taipei City 243, Taiwan (S.C. Chen).
E-mail address: chensc@mail.mcut.edu.tw (S.-C. Chen).
[1] These authors contributed equally to this work.

https://doi.org/10.1016/j.apsusc.2020.148264
Received 22 April 2020; Received in revised form 20 October 2020; Accepted 22 October 2020
Available online 26 October 2020

deposition, and sputtering deposition, have been utilized to grow thermoelectric thin films such as Bi_2Te_3, Sb_2Te_3 and Zinc antimonides [14–19]. Zinc antimonide is an alternative to PbTe-based thermoelectric materials. Due to its low cost, relatively large abundance, and low toxicity of Zn and Sb, it shows an overwhelming advantage in commercial applications in the temperature range (300–700 K) [20–22].

In the manufacturing process, most of Zn-Sb films need to be annealed to improve their thermoelectric properties. Being able to control the phase formation is hugely critical for tuning the TE properties of zinc antimonide [9,23,24]. After reviewing several literatures, it is found that the preparation of Zn-Sb alloy thin films by evaporation is seldom reported. In this paper, we applied ion beam assisted deposition technique in the e-gun evaporation process to improve the crystallinity, compactness and adhesion of the films. It is well known that the e-gun evaporator uses high-energy electron beam kinetic energy to convert the thermal energy required to melt the evaporation source, thereby heating the coating material in the crucible and depositing it smoothly on the substrate.

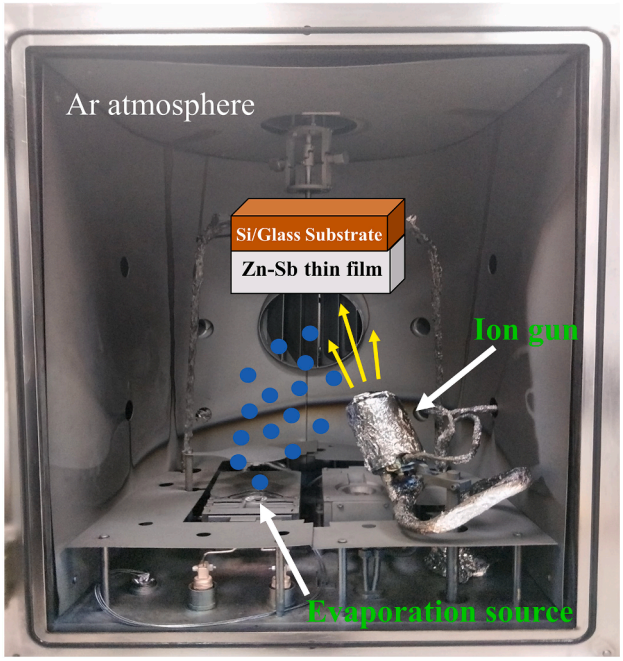

Fig. 1. The illustration of the evaporation process.

However, the atoms leaving the electron-beam melt usually only have a kinetic energy of 0.1–1 eV, which makes the deposited film structure loose, with the adhesion and compactness also poor. To improve the above disadvantages, we use an additional ion gun to assist in electron beam evaporation. The substrate can be cleaned by ion beam before film deposition. During deposition, it can be used to adjust the stoichiometry and structure of the films. The compactness of the films can also be improved by ion beam bombardment. Furthermore, the structure of the film and its corresponding thermoelectric properties will be discussed in depth in this article.

2. Experimental details

Zn-Sb alloy films all with thickness of 1000 nm were deposited on Corning 1737F glass by electron beam evaporation using an argon ion beam assisted deposition (IBAD) at room temperature. The base pressure was less than 5×10^{-6} torr and the working pressure was set at 1.5×10^{-4} torr with Ar of 5 sccm as the ion source. The Zn_4Sb_3 slugs served as the evaporation source. Fig. 1 shows an illustration of the evaporation process. The as-deposited samples were then annealed under argon gas atmosphere at 523 K for one hour and then water quenched to room temperature. The X-ray diffraction (XRD) patterns of Zn-Sb alloy films were collected by using x-ray diffraction diffractometer (PANalytical X'Pert Pro) with a Cu K_α X-ray radiation. The microstructures of the films were investigated by a scanning electron microscope (SEM, HITACHI S-3400N) and a transmission electron microscope (TEM, JEOL 2100F) with accelerating voltage of 200 kV. The chemical compositions of the films were characterized by the electron probe microanalyzer (EPMA JXA-8200, JEOL). The carrier concentrations of the films were measured by a Hall effect analyzer (AHM-800B, Agilent Technologies) with Van der Pauw's configuration. The Seebeck coefficient and electrical resistivity of films were measured using a commercially available instrument (ZEM-3, ULVAC-RIKO, Japan) under a helium atmosphere from room temperature to 550 K. The margin of error for the Seebeck coefficient and electrical conductivity measurement is 2–4%, while the margin of error for the power factor is ~10%. The X-ray photoelectron spectroscopic analysis (XPS) was performed using a Model Sigma Probe manufactured by Thermo VG-Scientific Company.

3. Results and discussion

The prepared Zn-Sb alloy films are usually heat-treated to improve their thermoelectric properties. The effects of heat treatment on the structural phase and crystallinity of Zn-Sb alloy films were investigated [25]. We found that when the annealing temperature is higher than 523

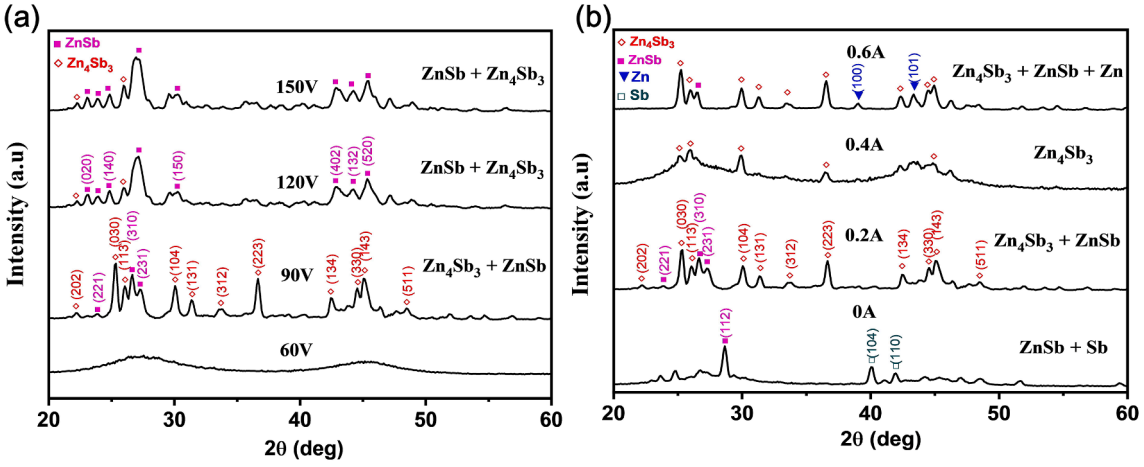

Fig. 2. XRD patterns of Zn-Sb films prepared by IBAD using (a) constant ion beam current (0.2 A) and varying ion beam voltage, (b) constant ion beam voltage (90 V) and varying ion beam current.

K, the film has remarkable crystallinity in the mixture of Zn_4Sb_3 and ZnSb phases. In all experiments of varying ion voltages and currents, the films' deposition rate was 6 Å/s and all films were subjected to a heat treatment process at 523 K for one hour, and then cooled down to room temperature by water quenching.

It is known that ion source energy can be altered by adjusting the anode voltage or current. When the energy of the ion beam is increased; namely, when the bombardment energy is increased, the kinetic energy of the deposited molecules can be increased. In turn, the generation of pores and columnar structures can be reduced. In contrast, if the ion energy becomes too high, it will cause the deposited molecules to be blown out and collide with other molecules that are being subsequently deposited. Thus, the mobility and kinetic energy of the deposited molecules on the other hand will diminish, which will result in a decrease in the bulk density of the film. To optimize the effect of IBAD on the structure of Zn-Sb alloy thin films, a systematic study of XRD analysis has been carried out. In Fig. 2a, all films were prepared by setting a constant ion beam current (0.2 A) and changing the ion beam voltage. It can be seen that when the Ar ion beam voltage is set at 90 V, the crystalline phase is a mixed phase of Zn_4Sb_3 + ZnSb, and has good crystallinity. When the Ar ion beam voltage is raised to 120 V, the phase structure with a mixed phase of ZnSb + Zn_4Sb_3 still exists, but the ZnSb phase becomes the dominant phase. By adjusting the voltage of the Ar ion beam we can easily alter the bombardment energy of the ion beam, resulting in a significant change in the phase structure of the film layer. Excessive Ar ion beam voltage will cause the film's crystallinity to deteriorate due to the bombardment energy being too large. We also found that as the ion beam voltage increases, the grain size calculated from Scherrer equation will decrease from 20.3 nm to 13.9 nm. When the Ar ion beam voltage is set at 90 V, the optimal ion gun bombardment energy is obtained.

We further investigated the effect of Ar ion beam current on the film

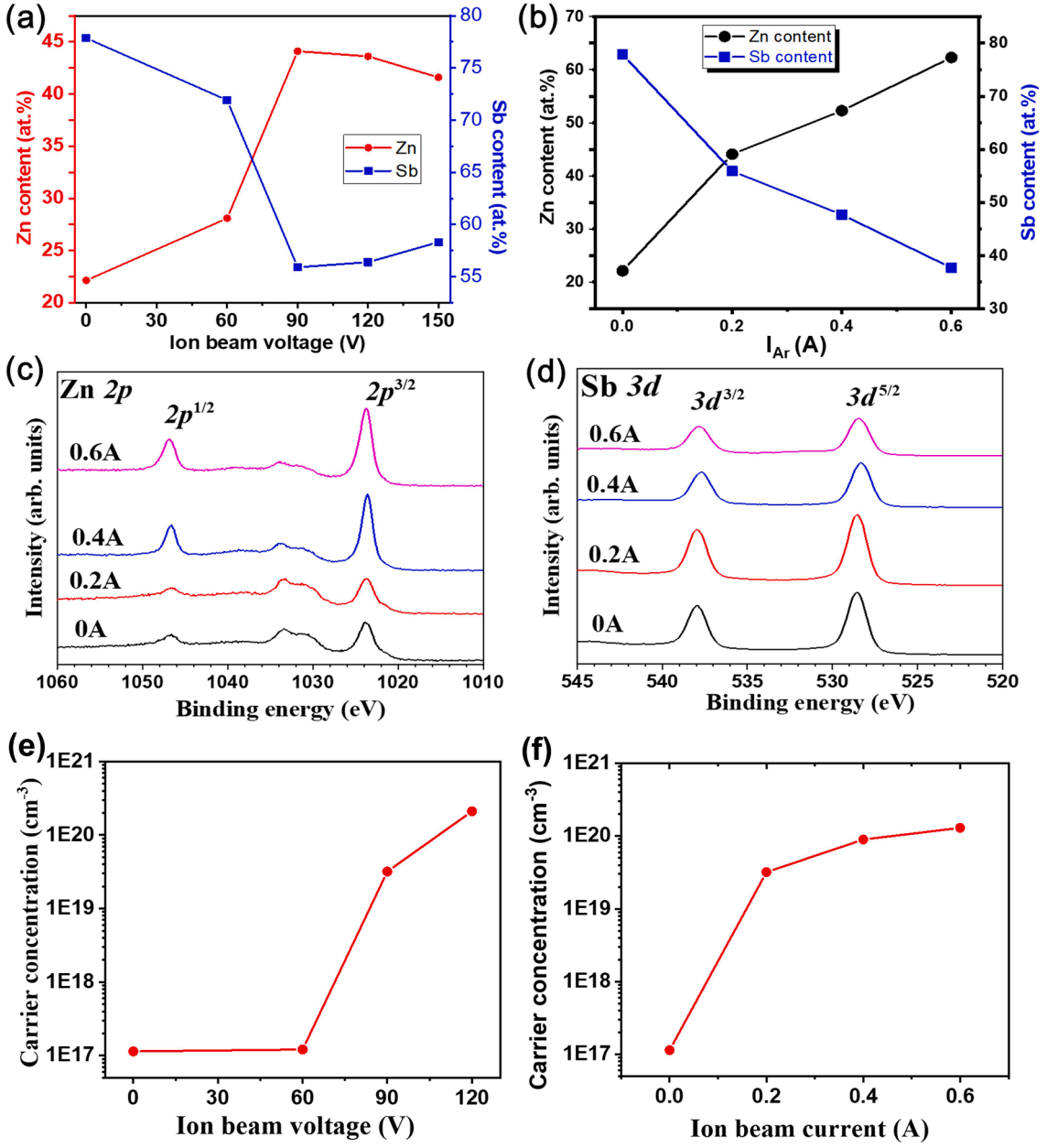

Fig. 3. Elemental composition, XPS analysis and carrier concentrations of Zn-Sb films: (a) fixed Ar ion beam current at 0.2 A, varying Ar ion beam voltage, (b) fixed Ar ion beam voltage at 90 V , varying Ar ion beam current, (c) XPS spectra of Zn *2p* core level of Zn-Sb films, (d) XPS spectra of Sb *3d* core level of Zn-Sb films, (e) the relationship between carrier concentration and ion beam voltage, (f) the relationship between carrier concentration and ion beam current.

structure. Fig. 2b is the XRD graph of fixed Ar ion beam voltage (90 V) and varying Ar ion beam current in the range of 0–0.6 A. When the ion beam current is set at 0.2 A, the film shows a mixed phase of Zn_4Sb_3 + ZnSb. As the ion beam current rises to 0.6 A, a new crystalline phase of Zn peak (1 0 1) appears. It can be seen that as the Ar ion beam current increases, the crystalline phase will gradually change from the original ZnSb + Sb mixed phase to the Zn_4Sb_3 + ZnSb + Zn mixed phase. We believe that because the melting point and boiling point of Zn are relatively lower than Sb, it is easy to vaporize Zn at low pressures. Therefore, the increase of the current through the Ar ion beam will greatly increase the probability of bombardment, which will cause Zn to be more easily deposited on the substrate.

Fig. 3 shows the detailed analysis of elemental composition, chemical binding environment and carrier concentrations of Zn-Sb films deposited by electron beam evaporation through IBAD technology under different conditions. Fig. 3a is the composition diagram of when the Ar ion beam current was fixed at 0.2 A and the Ar ion beam voltage is changed from 0 to 150 V. We can see that as the voltage of the argon ion beam increases, the content of Zn gradually increases, while the content of Sb decreases. This is because the energy of the ion beam bombardment in the film rises, which then introduces more Zn to change the phase structure. Fig. 3b is a composition diagram of when the Ar ion beam voltage is fixed at 90 V and the Ar ion beam current is varied from 0 to 0.6 A. It can be observed that with the increase of the Ar ion beam current, the content of Zn also rises, while the content of Sb decreases. Due to the increase of Zn content, the phase structure gradually changes from ZnSb + Sb mixed phase to form Zn_4Sb_3 + ZnSb + Zn mixed phase. Our results indicate that ion beam currents of 0.2 and 0.6 A can provide a suitable condition for the preparation of mixed phase films with more uniform and dense grain distribution. According to previous reports [23], a more dense and uniform thin film formed from the Zn_4Sb_3 phase will have better thermoelectric properties. Therefore, from the above composition analysis results, we have proved that both the voltage and current of the Ar ion beam will affect the film's structure phase and composition. In addition, the binding energies of Zn *2p* and Sb *3d* core levels of a series of Zn-Sb films are presented in Fig. 3c and d. It can be seen that the peak intensity of Zn *2p* becomes stronger, and the binding energy of $3d^{5/2}$ shifts to a lower value upon increasing the ion beam current. In other words, when there is a higher ion beam current assisted deposition, more Zn content and more negatively charged Sb will exist in the film [26]. This also explains how Zn_4Sb_3 gradually transforms in the main crystalline phase in the film as the ion beam current increases. Overall, these results have confirmed that the structural phase and composition of the film can indeed be effectively controlled by the voltage and current of the ion beam. As a result, the carrier transport characteristics of the films should have also been regulated. Fig. 3e and f present the relationship between carrier concentration and ion beam parameters. On the whole, suitable ion beam parameters can adjust the carrier concentration of the film to the range of about 10^{19}–10^{20} cm^{-3} to ensure the best thermoelectric properties.

Figs. 4 and 5 show the surface morphology of the Zn-Sb alloy thin films produced under various deposition conditions. Fig. 4 is the SEM image of varying the Ar ion beam voltage from 0 to 150 V. We can see that as the voltage of the ion beam increases, the surface particles become uniform and dense, which is caused by the ions bombarding the film layer to achieve an annealing-like effect. Fig. 5 shows the SEM image of varying Ar ion beam current from 0 to 0.6 A. It can be found that as the ion beam current rises, the surface morphology and particles gradually become more dense and larger. It is worth noting that when the ion beam current is set at 0.2 A, a mixed phase film that is more uniform and dense is achieved. The higher ion beam current leads to the formation of the metal phase Zn. Generally, the films that form Zn_4Sb_3 phase with more dense and uniform particles possess better electrical conductivity.

We measured the temperature dependence of Seebeck coefficient and electrical conductivity of films to study their thermoelectric properties, as shown in Fig. 6 (a) and (b). All the films show p-type characteristics (Fig. 6a). Generally speaking, materials with lower carrier concentrations will have larger Seebeck coefficients. For the Zn-Sb film without ion-beam assisted deposition in this work, having a higher Seebeck coefficient is consistent with the result of carrier concentration measurement presented in Fig. 3f. The electrical conductivity of all films increased with increasing temperature, indicating their semiconducting properties (Fig. 6b). In particular, the thin film with Zn_4Sb_3 + ZnSb mixed phase exhibits a higher electrical conductivity and a better Seebeck coefficient in higher temperature regions. The simultaneous increase in electrical conductivity and Seebeck coefficient actually contribute to a significant increase in power factor. For the films made with 0.6 A ion beam current, a relatively high power factor was obtained. The maximum power factor at 550 K can be as high as ~1280 μW/m-K^2 (Fig. 6c), which is almost comparable to the recently published record [24,27,28]. It is generally known that ZnSb phase has a high Seebeck coefficient and electrical conductivity with high thermal conductivity, whereas Zn_4Sb_3 phase has a low thermal conductivity and a small Seebeck coefficient and electrical conductivity. A material with both ZnSb and Zn_4Sb_3 mixed phases might exhibit the advantages of both phases, which could result in enhanced thermoelectric properties. The results therefore clearly indicate that as long as a film has a mixed

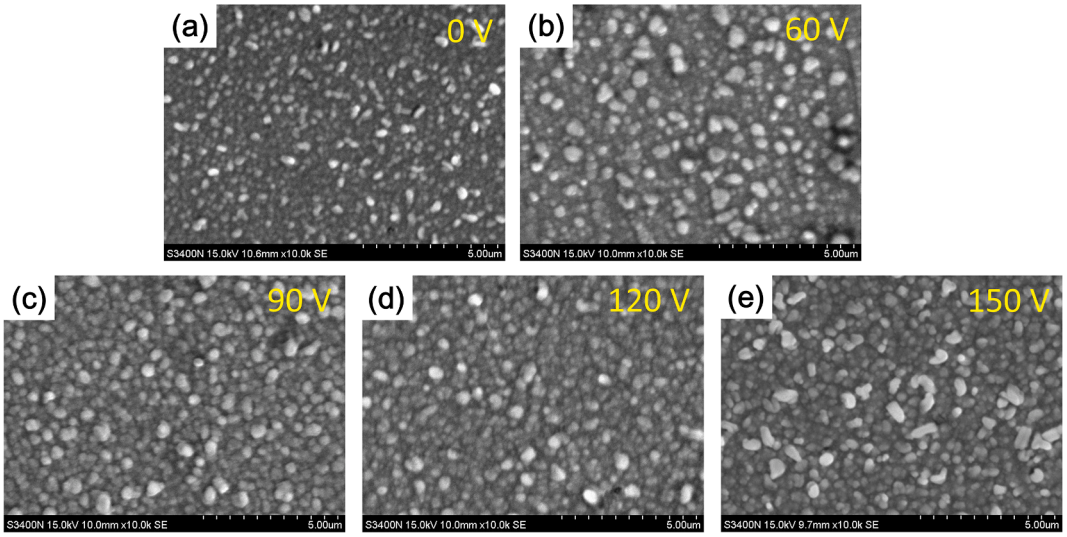

Fig. 4. SEM images of varying Ar ion beam voltage with the Ar ion beam current fixed at 0.2 A.

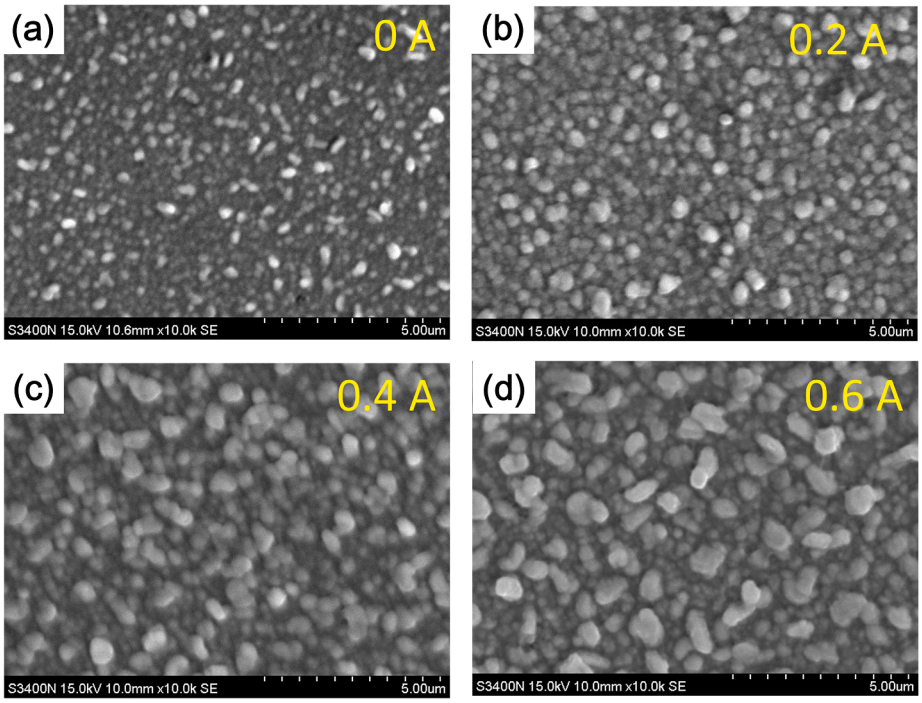

Fig. 5. SEM images of varying Ar ion beam current with the Ar ion beam voltage fixed at 90 V.

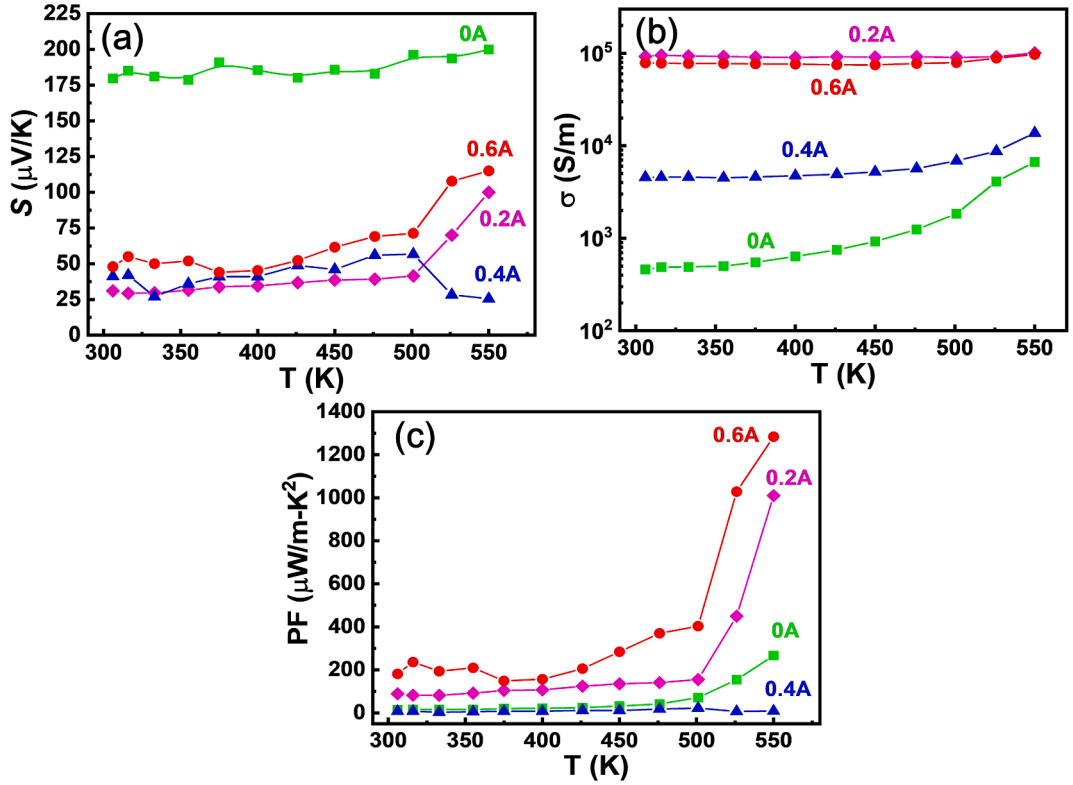

Fig. 6. Temperature dependence of (a) Seebeck coefficient, (b) electrical conductivity, and (c) power factor for the Zn-Sb films prepared by IBAD by varying the ion beam current and fixing the ion beam voltage at 90 V.

phase of ZnSb and Zn_4Sb_3, it will have better thermoelectric properties than a film with only Zn_4Sb_3 single phase (I_{Ar} = 0.4 A) or ZnSb + Sb mixed phase (I_{Ar} = 0 A). In addition, we also observed in detail the microstructure of the best film (I_{Ar} = 0.6 A) by high-resolution transmission electron microscopy (HRTEM) to understand the factors that may affect its thermoelectric transporting properties. From the HRTEM images presented in Fig. 7, we can clearly observe the grain and phase boundaries, and the distribution of Zn nano-inclusion in the ZnSb matrix. Generally speaking, these unique nanostructures and interfaces will help to significantly reduce the thermal conductivity of the film and further enhance its TE performance.

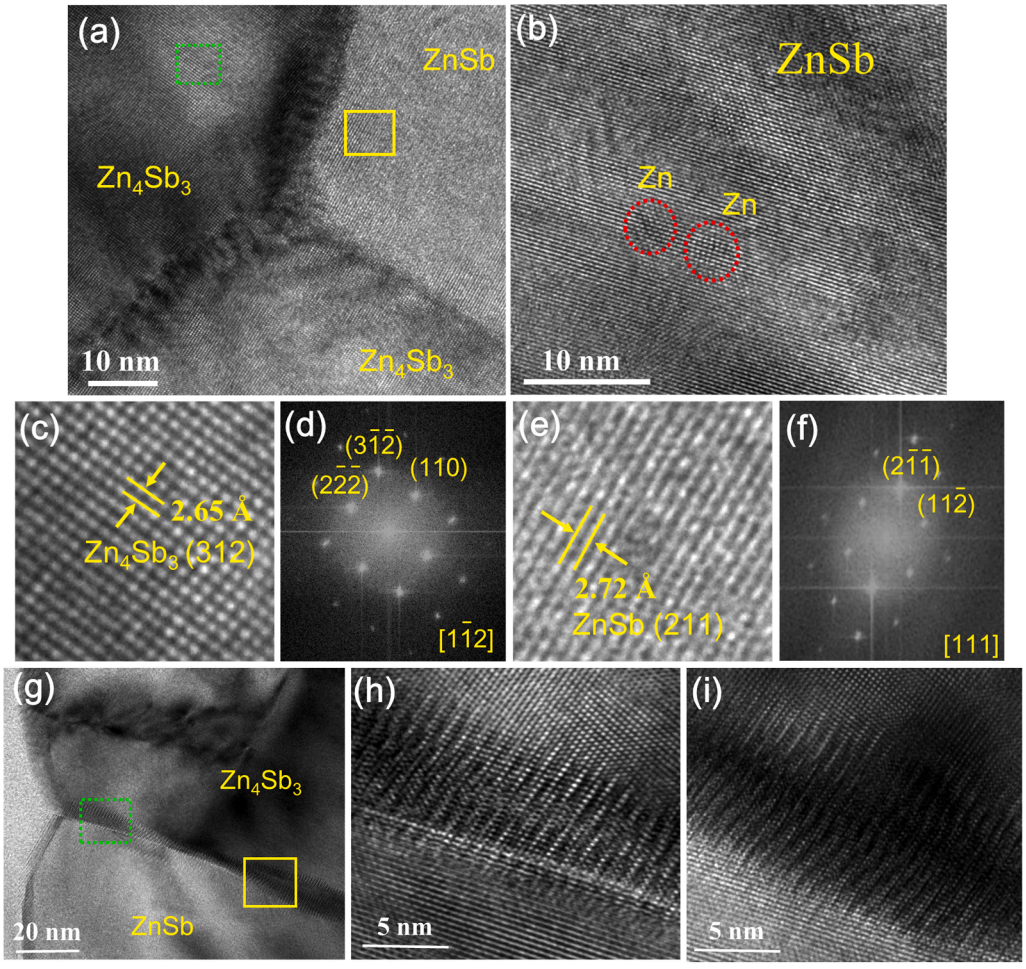

Fig. 7. Bright-field TEM images of Zn-Sb film deposited with the ion beam voltage/current set at 90 V/0.6A. (a) HRTEM image showing grain and phase boundaries. (b) HRTEM image of Zn nanoparticles embedded in the ZnSb matrix. (c) Enlarged view of dotted green boxed region in panel a. (d) The fast Fourier transformation image of panel c. (e) Enlarged view of solid yellow boimages of varying Ar ion beam current xed region in panel a. (f) The fast Fourier transformation image of panel e. (g) HRTEM micrograph shows the boundaries between two structural phases. (h) Enlarged view of dotted green boxed region in panel g. (i) Enlarged view of solid yellow boxed region in panel g. (For interpretation of the references to colour in this figure legend, the reader is referred to the web version of this article.)

4. Conclusion

In summary, we have demonstrated that Zn-Sb alloy films can successfully be prepared by electron beam evaporation through an ion beam assisted deposition. From the analysis of XRD and XPS and the results of thermoelectric measurements, it can be seen that when the ion beam voltage is set at 90 V and the current is set at 0.2 or 0.6 A, a film with a mixed phase of Zn_4Sb_3 + ZnSb and excellent thermoelectric properties will be produced. A high power factor value of ~1280 μW/m-K^2 is obtained in the films assisted by an ion beam current of 0.6 A, showing a greater improvement than that of the single phase. Controlling the structural phase and crystallinity is an effective strategy to improve the thermoelectric properties in zinc antimonide films.

CRediT authorship contribution statement

Shih-Chieh Hsu: Investigation. **Jhen-Yong Hong:** Investigation. **Cheng-Lung Chen:** Investigation. **Sheng-Chi Chen:** Conceptualization, Methodology. **Jia-Han Zhen:** Formal analysis. **Wen-Pin Hsieh:** Resources. **Yang-Yuan Chen:** Resources. **Tung-Han Chuang:** Conceptualization, Methodology.

Declaration of Competing Interest

The authors declare that they have no known competing financial interests or personal relationships that could have appeared to influence the work reported in this paper.

Acknowledgements

We gratefully acknowledge the Ministry of Science and Technology of Taiwan (grant Nos. 107-2221-E-131-036 and 108-2221-E-032-031) and the Academia Sinica research grant (AS-SS-109-01-110) for their financial support. We also thank Prof. H.C. Lin and Mr. C.Y. Kao of the Instrumentation Center, National Taiwan University for their assistance with EPMA experiments.

References

[1] R. Venkatasubramanian, E. Siivola, T. Colpitts, B. O'Quinn, Thin-film thermoelectric devices with high room-temperature figures of merit, Nature 413 (2001) 597–602.
[2] T.M. Tritt, M.A. Subramanian, Thermoelectric materials, phenomena, and applications: a bird's eye view, MRS Bull. 31 (2006) 188–198.
[3] G.J. Snyder, E.S. Toberer, Complex thermoelectric materials, Nat. Mater. 7 (2008) 105–114.
[4] G.J. Tan, L.D. Zhao, M.G. Kanatzidis, Rationally designing high-performance bulk thermoelectric materials, Chem. Rev. 116 (2016) 12123–12149.
[5] H.S. Kim, W.S. Liu, G. Chen, C.W. Chu, Z.F. Ren, Relationship between thermoelectric figure of merit and energy conversion efficiency, Proc. Natl. Acad. Sci. U.S.A. 112 (2015) 8205–8210.
[6] F.J. Zhang, Y.P. Zang, D.Z. Huang, C.A. Di, D.B. Zhu, Flexible and self-powered temperature-pressure dual-parameter sensors using microstructure-frame-supported organic thermoelectric materials, Nat. Commun. 6 (2015) 8356.
[7] Z.G. Chen, G. Han, L. Yang, L.N. Cheng, J. Zou, Nanostructured thermoelectric materials: current research and future challenge, Prog. Nat. Sci. 22 (2012) 535–549.
[8] W.S. Liu, Q. Jie, H.S. Kim, Z.F. Ren, Current progress and future challenges in thermoelectric power generation: from materials to devices, Acta Mater. 87 (2015) 357–376.
[9] P.Y. Lee, P.H. Lin, Evolution of thermoelectric properties of Zn_4Sb_3 prepared by mechanical alloying and different consolidation routes, Energies 11 (2018) 1200.

[10] K. Biswas, J.Q. He, I.D. Blum, Chun-Iwu, T.P. Hogan, D.N. Seidman, V.P. Dravid, M.G. Kanatzidis, High-performance bulk thermoelectrics with all-scale hierarchical architectures, Nature 489 (2012) 414–418.
[11] Y.Z. Pei, X.Y. Shi, A. LaLonde, H. Wang, L.D. Chen, G.J. Snyder, Convergence of electronic bands for high performance bulk thermoelectrics, Nature 473 (2011) 66–69.
[12] S.J. Kim, J.H. We, B.J. Cho, A wearable thermoelectric generator fabricated on a glass fabric, Energ. Environ. Sci. 7 (2014) 1959–1965.
[13] W.H. Zhang, J.K. Yang, D.Y. Xu, A high power density Micro-thermoelectric generator fabricated by an integrated bottom-up approach, J. Microelectromech. Syst. 25 (2016) 744–749.
[14] C.V. Manzano, A.A. Rojas, M. Decepida, B. Abad, Y. Feliz, O. Caballero-Calero, D. A. Borca-Tasciuc, M. Martin-Gonzalez, Thermoelectric properties of Bi_2Te_3 films by constant and pulsed electrodeposition, J. Solid State Electr. 17 (2013) 2071–2078.
[15] E.M.F. Vieira, J. Figueira, A.L. Pires, J. Grilo, M.F. Silva, A.M. Pereira, L. M. Goncalves, Enhanced thermoelectric properties of Sb_2Te_3 and Bi_2Te_3 films for flexible thermal sensors, J. Alloys Compd. 774 (2019) 1102–1116.
[16] J.H. Kim, J.Y. Choi, J.M. Bae, M.Y. Kim, T.S. Oh, Thermoelectric characteristics of n-Type Bi_2Te_3 and p-Type Sb_2Te_3 thin films prepared by co-evaporation and annealing for thermopile sensor applications, Mater. Trans. 54 (2013) 618–625.
[17] B. Fang, Z.G. Zeng, X.X. Yan, Z.Y. Hu, Effects of annealing on thermoelectric properties of Sb_2Te_3 thin films prepared by radio frequency magnetron sputtering, J. Mater. Sci. Mater. Electron. 24 (2013) 1105–1111.
[18] X. Wang, H.C. He, N. Wang, L. Miao, Effects of annealing temperature on thermoelectric properties of Bi_2Te_3 films prepared by co-sputtering, Appl. Surf. Sci. 276 (2013) 539–542.
[19] X. Bo, A.Y. Tang, M.L. Dou, Z.L. Li, F. Wang, Controllable electrodeposition and mechanism research of nanostructured Bi_2Te_3 thin films with high thermoelectric properties, Appl. Surf. Sci. 486 (2019) 65–71.
[20] Y. Sun, M. Christensen, S. Johnsen, N.V. Nong, Y. Ma, M. Sillassen, E. Zhang, A.E. C. Palmqvist, J. Bottiger, B.B. Iversen, Low-cost high-performance zinc antimonide thin films for thermoelectric applications, Adv. Mater. 24 (2012) 1693–1696.
[21] Z.H. Zheng, P. Fan, J.T. Luo, G.X. Liang, P.J. Liu, D.P. Zhang, Enhanced thermoelectric properties of Cu doped ZnSb based thin films, J. Alloys Compd. 668 (2016) 8–12.
[22] A. Bellucci, M. Mastellone, M. Girolami, S. Orlando, L. Medici, A. Mezzi, S. Kaciulis, R. Polini, D.M. Trucchi, ZnSb-based thin films prepared by ns-PLD for thermoelectric applications, Appl. Surf. Sci. 418 (2017) 589–593.
[23] Z.H. Zheng, P. Fan, P.J. Liu, J.T. Luo, G.X. Liang, D.P. Zhang, Zinc antimonide thin films prepared by ion beam sputtering deposition using ternary layers annealing method, J. Alloy Compd. 594 (2014) 122–126.
[24] P.P. Murmu, S.V. Chong, J. Storey, S. Rubanov, J. Kennedy, Secondary phase induced electrical conductivity and improvement in thermoelectric power factor of zinc antimonide films, Mater. Today Energy 13 (2019) 249–255.
[25] X. Song, M. Schrade, N. Maso, T.G. Finstad, Zn vacancy formation, Zn evaporation and decomposition of ZnSb at elevated temperatures: influence on the microstructure and the electrical properties, J. Alloys Compd. 710 (2017) 762–770.
[26] D. Tang, W. Zhao, S. Cheng, P. Wei, J. Yu, Q. Zhang, Crystal structure and bonding characteristics of In-doped β-Zn_4Sb_3, J. Solid State Chem. 193 (2012) 89–93.
[27] Z.H. Zheng, P. Fan, P.J. Liu, J.T. Luo, X.M. Cai, G.X. Liang, D.P. Zhang, F. Ye, Y. Z. Li, Q.Y. Lin, Enhanced thermoelectric properties of mixed zinc antimonide thin films via phase optimization, Appl. Surf. Sci. 292 (2014) 823–827.
[28] P.J. Liu, A.H. Zhong, M.M. Yin, Z.H. Zheng, P. Fan, The thermoelectric properties of zinc antimonide thin films fabricated through single element composite target, Surf. Coat. Technol. 361 (2019) 130–135.